Iris Recognition: An Analysis of the Aliasing Problem in the Iris Normalization Stage

Hugo Proença and Luís A. Alexandre
Dep. Informatics, IT - Networks and Multimedia Group
Universidade da Beira Interior, Covilhã, Portugal
Email: {hugomcp,lfbaa}@di.ubi.pt

Abstract

Iris recognition has been increasingly used with very satisfactory results. Presently, the challenge consists in unconstrain the image capturing conditions and enable its application to domains where the subjects' cooperation is not expectable (e.g. criminal/terrorist seek, missing children). In this type of use, due to variations in the image capturing distance and in the lighting conditions that determine the size of the subjects' pupil, the area correspondent to the iris in the captured images will be highly varying too. In order to compensate this variation, common iris recognition proposals translate the segmented iris image to a double dimensionless pseudo-polar coordinate system, in a process known as the normalization stage, which can be regarded as a sampling of the original data with the inherent possibility of aliasing. In this paper we analyze the relationship between the size of the captured iris image and the overall recognition's accuracy. Further, we identify the threshold for the sampling rate of the iris normalization process above which the error rates significantly increase.

Keywords: iris normalization, aliasing, iris recognition, biometrics.

1. Introduction

In 1987, L. Flom and A. Safir estimated at 1 in 10^{72} the probability for the existence of two similar irises and concluded about the stability of iris morphology over human lifetime. Since then, the use of the iris as biometric measure has been increasingly encouraged by both government and private entities. Iris is commonly recognized as one of the most reliable biometric signals: it has a random morphogenesis and apparently no genetic penetrance.

From our viewpoint, the present challenge consists in achieve accurate iris recognition in less constrained image capture environments, either under natural luminosity, from different image capturing distances and without users' cooperation.

In order to achieve invariance to the varying size of the pupil and to the distance and angle of the image capturing framework, common iris recognition proposals apply a normalization process to the segmented iris. The translation to a double dimensionless pseudo-polar coordinate system with fixed dimensions can be regarded as a sampling process, with the inherent possibility of aliasing that deteriorates the recognition's accuracy.

Given a power spectrum (a plot of power versus frequency), aliasing is a false translation of power falling in some frequency range $(-f_c, f_c)$ outside the range. It can be caused by discrete sampling below the Nyquist frequency and causes that different signals could become indistinguishable when sampled. When this happens, the original signal cannot be uniquely reconstructed from the sampled signal.

In this paper we analyze the relationship between the size of the captured iris images and the iris recognition's accuracy, regarding the probability of aliasing in the normalization stage. We selected two highly dissimilar iris image data sets (UBIRIS [6] and UPOL [3]) and analyzed the results obtained by the classical Daugman's recognition method [2], when varying the size of the captured iris images. It will be shown that when the area correspondent to the iris in the captured image is below 30% of the size of the normalized one, it occurs a large deterioration in the recognition accuracy, specially due to a substantial increase of the false rejections.

The remainder of this paper is organized as follows: section 2 briefly summarizes the most cited iris recognition methods. A detailed description of two common iris normalization proposals is given in section 2.2. Section 3 reports the experiments and results and, finally, section 4 concludes this paper.

2. Iris Recognition

2.1. Overview

In spite of the specificities from distinct proposals, typical iris recognition systems share the common structure illustrated by figure 1.
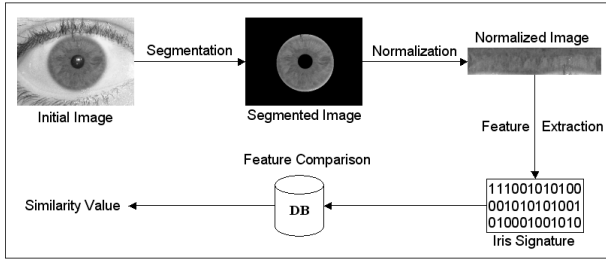

Figure 1. Typical iris recognition stages

The initial stage deals with iris segmentation. This consists in localize the iris inner (pupillary) and outer (scleric) borders. There are two major strategies for iris segmentation: to use a rigid or deformable template of the iris or its boundary. In most cases, the boundary approach is very similar to the proposed by Wildes [9]: it begins by the construction of an edges map followed by the application of some geometric form fitting algorithm. Authors of [7] used this strategy together with a clustering process to increase the accuracy in noisy environments. The template-based strategies usually involve the maximization of some equation, as proposed by Daugman [2]:

In order to compensate the varying size of the captured iris it is common to translate the segmented iris region, represented in the cartesian coordinate system, to a fixed length and dimensionless polar coordinate system. This is usually accomplished through a method similar to the Daugman's Rubber Sheet [2].

The next stage is the feature extraction. From this viewpoint, iris recognition approaches can be classified into three major categories: phase-based methods (e.g. [2]), zero crossing methods (e.g. [1]) and texture analysis based methods (e.g [9]).

In the final stage it is made a comparison between iris signatures, producing a numeric dissimilarity value. If this value is higher than a threshold, the system outputs a "non-match", meaning that each signature belongs to different irises. Otherwise, the system outputs a "match", meaning that both signatures were extracted from images of the same iris. Different metrics like the Hamming, Euclidean, Weighted Euclidean or methods based on signal correlation (e.g. [9]) can be applied.

2.2. Iris Normalization Methods

Robust representations for pattern recognition must be invariant to changes in the size, position and orientation of the patterns. In the iris biometric compass, this means that a representation of the iris data invariant to changes in the distance between the eye and the capturing device, in the camera optical magnification factor and in the iris orientation, caused by torsional eye rotation and camera angles, must be accomplished. As described in [2], the invariance to all of these factors can be achieved by the translation of the captured data to a double dimensionless pseudo-polar coordinate system. Figure 2 illustrates the translation process, that is based in a polar (θ) and radial (r) variables. "i" and "p" represent respectively the center of the iris and of the pupil and (o_x, o_y) the difference between both centers. The normalization is anti-clockwise processed, extracting a fixed number of pixels from circumferences with successive radius values, into the normalized rectangular image with fixed dimensions.
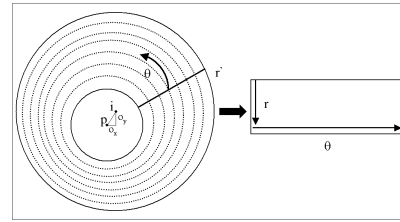

Figure 2. Iris Normalization [2].

Formally, the rubber sheet is a linear model that assigns to each pixel of the iris, regardless its size and pupillary dilation, a pair of real coordinates (r, θ), where r is on the unit interval [0, 1] and θ is an angle in [0, 2π]. The remapping of the iris image $I(x, y)$ from raw cartesian coordinates (x, y) to the dimensionless non concentric polar coordinate system (r, θ) can be represented as:

$$I(x(r, \theta), y(r, \theta)) \rightarrow I(r, \theta) \quad (1)$$

where $x(r, \theta)$ and $y(r, \theta)$ are defined as linear combinations of both the set of pupillary boundary points $(x_p(\theta), y_p(\theta))$ and the set of limbus boundary points along the outer perimeter of the iris $(x_s(\theta), y_s(\theta))$ bordering the sclera:

$$\begin{cases} x(r, \theta) = (1 - r) * x_p(\theta) + r * x_s(\theta) \\ y(r, \theta) = (1 - r) * y_p(\theta) + r * y_s(\theta) \end{cases} \quad (2)$$

Authors of [10] proposed a slightly different iris normalization model, which combines linear and non-linear methods to unwrap the iris region. They start by performing a non-linear transformation of all iris patterns to a reference annular zone with a predefined ratio of the radii of inner and

outer boundaries of the iris. Further, this reference annular zone is linearly unwrapped to a fix-sized rectangle block for subsequence processing. Both normalization processes can be regarded as point sampling operators of the original image I defined by $s(I) = (I(t_1), I(t_2), \ldots, I(t_n))$, $t_i = \frac{i}{n}$, $i = 1, \ldots, n$

2.3. Aliasing

Let I_1 and I_2 be two iris images similar to the "Initial Image" of figure 1. Also, let $A(I)$ denote the area correspondent to the iris in image I ("Segmented Image" of figure 1). In the normalization stage (s), as in any other point sampling process, aliasing can occur in two distinct forms:

- I_1 and I_2 are very dissimilar and $s(I_1)$ and $s(I_2)$ are highly similar. In the iris biometric compass, this will increase the false accept rate (FAR).

- I_1 and I_2 are very similar and $s(I_1)$ and $s(I_2)$ are are highly dissimilar, increasing the false rejection rate (FRR).

Commonly, the normalized iris images have fixed dimensions of 512×64 pixels, respectively in the angular and radial directions, thus $A(s(I)) = 32768$ pixels. The sampling rate r of the normalization process s can be given by:

$$r = \frac{A(s(I))}{A(I)} = \frac{32768}{A(I))} \qquad (3)$$

where I is the captured iris image. In our experiments, we varied the size of the captured iris image ($A(I)$) and analyzed its influence in the overall accuracy of iris recognition. It will be shown that when $r > 4$ there is a strong increase of the recognition error rates, induced by the aliasing occurred in the normalization process.

3. Experiments

In the experiments, we implemented the method described by Daugman [2] which is composed by four main stages. In the segmentation we implemented the integrodifferential that searches for both iris borders. Feature extraction was accomplished through the use of two dimensional Gabor filters followed by a binarization process. Finally, feature comparison was made through the Hamming distance.
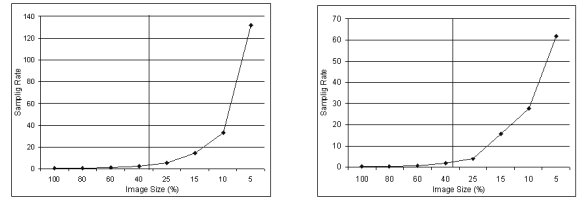
3.1. Data Sets

There are presently 5 public and free available iris image databases for biometric purposes: CASIA [4], MMU [5], BATH [8], UPOL [3] and UBIRIS [6].

Based in the databases characteristics, we selected 130 images from $UBIRIS$ and $UPOL$ databases, in order to analyze the recognition accuracy both in noisy and noise-free environments. Images from $UBIRIS$ database have (800×600) pixels and average pupil and iris radius of respectively 51 and 185 pixels, which gives an average iris area of 99437 pixels and 0.3298 for the average sampling rate of the normalization process. Regarding the images from the $UPOL$ data set, they have 768×576 pixels, pupil and iris radius with respectively 69 and 271 pixels, 215758 of average iris area and 0.1518 for the average sampling rate.

In order to avoid that segmentation errors corrupt the obtained results, we manually verified that the segmentation algorithm accurately segmented all the images from both data sets. The simulation of the different sizes of the captured iris images was accomplished through bi-cubic resizing of the original images of the data sets. Each image was resized from 100% to 10% of its original size.

3.2. Results

(a) Average sampling rate (r) from the images of $UBIRIS$ data set.

(b) Average sampling rate (r) from the images of $UPOL$ data set.

Figure 3. Average sampling rate (r) of the normalization process.

According to (3), figure 3 contains the average sampling rate of the normalization processes in the images from $UBIRIS$ (figure 3a) and $UPOL$ (figure 3b) data sets as the dimension of the captured iris images varies. The horizontal axis specifies the size of the captured iris images proportionally to the initial images size (values are percent). The vertical axis contains the average sampling rate (r) of the normalization processes of these images.

Figure 4 contains four measures of the recognition's accuracy regarding the size of the images presented to the segmentation algorithm. The solid lines represent the results obtained in the $UBIRIS$ data set and the dashed line represents the results obtained in the $UPOL$ data set. One again, the horizontal axis denotes the size of the used images in proportion (percentage) with the average dimension
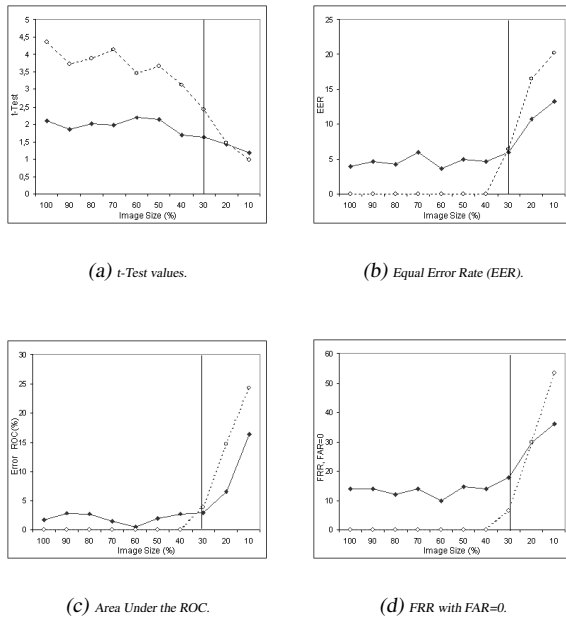
(a) t-Test values.

(b) Equal Error Rate (EER).

(c) Area Under the ROC.

(d) FRR with FAR=0.

Figure 4. Recognition's accuracy regarding the size of the images presented to the segmentation algorithm.

4. Conclusions

In this paper we analyzed the influence of the sampling rate of the iris normalization stage in the overall accuracy of iris recognition.

We observed no significant degradation in the accuracy when the sampling rates are lower than 5. For higher sampling rates (correspondent to original images with iris area below 30% of the normalized one), the error rates significantly increase.

This fact indicates a strong probability of aliasing when iris images are captured at a distance. From our viewpoint, the increase of the error rates, specially the false rejections, requires alternate sampling/normalization processes more tolerant to highest variations in the size of the captured iris images. Moreover, we stress that the observed deterioration in the recognition's accuracy is independent of the amount of noise that the iris region contain, since the values obtained for the minimum demandable sampling rates in the $UBIRIS$ (noisy images) and in the $UPOL$ (high quality images) data sets were approximately equal.

of the images.. The vertical line corresponds to the identified threshold of 30%, from which the error rates significantly increase. Figure 4a contains the values for a t-test given by $\tau = (\mu_E - \mu_I)/\sqrt{\frac{\sigma_I{}^2}{N_I} + \frac{\sigma_E{}^2}{N_E}}$, where symbols μ_I and μ_E respectively indicate the means of the intra- (images from the same iris) and inter-class (images from different irises) comparisons. σ_I and σ_E indicate the respective standard deviations and N_I and N_E the total intra- and inter-class comparisons.

Figure 4b contains the equal error rates and figure 4c the percent values for the areas under the receiver operating curves (ROC). Finally, figure 4d contains the values of the false rejections when the false acceptances are minimized.

We observed that the separability between the intra- and inter-class comparisons remained with similar values until the iris area in the captured image is below 40% of the normalized image one, either in the $UBIRIS$ and in the $UPOL$ data sets. Moreover, when the area of the original data is below 30% of the normalized one there is a significant decrease in the separability between the intra- and inter-class comparisons, corresponding to sampling rates (3) higher than 5. Above this value we observed a significant increment of the error rates, specially the false rejections, allowing the conclusion of aliasing in the iris normalization stage.

References

[1] W. W. Boles and B. Boashash. A human identification technique using images of the iris and wavelet transform. *IEEE Transactions on Signal Processing, vol. 46, no. 4*, pages 1185–1188, April 1998.

[2] J. G. Daugman. High confidence visual recognition of persons by a test of statistical independence. *IEEE Transactions on Pattern Analysis and Machine Intelligence, Vol. 25, No. 11*, pages 1148–1161, November 1993.

[3] M. Dobes and L. Machala. UPOL iris image database, 2004. http://phoenix.inf.upol.cz/iris/

[4] Institute of Automation, Chinese Academy of Sciences. CASIA iris image database, 2004. http://www.sinobiometrics.com

[5] Multimedia University. MMU iris image database, 2004. http://pesona.mmu.edu.my/ccteo

[6] H. Proença and L. A. Alexandre. UBIRIS: A noisy iris image database. In *13th International Conference on Image Analysis and Processing (ICIAP2005)*, pages 970–977, September 2005. http://iris.di.ubi.pt

[7] H. Proença and L. A. Alexandre. Iris segmentation methodology for non-cooperative iris recognition. *IEE Proc. Vision, Image & Signal Processing, vol. 153, issue 2*, pages 199–205, 2006.

[8] University of Bath. University of Bath iris image database, 2004. www.bath.ac.uk/elec-eng/pages/sipg/

[9] R. P. Wildes. Iris recognition: an emerging biometric technology. In *Proceedings of the IEEE, vol. 85, no.9*, pages 1348–1363, U.S.A., September 1997.

[10] X. Yuan and P. Shi. A non-linear normalization model for iris recognition. In *Proceedings of the International Workshop on Biometric Recognition Systems IWBRS 2005*, pages 135–142, China, 2005.